Mode of action of cyclic imine toxins: 20-methyl spirolide-G antagonizes rat neuronal $\alpha 3\beta 2$ nicotinic acetylcholine receptor

Amandine Gaudin, Rómulo Aráoz

Mode of action of cyclic imine toxins: 20-methyl spirolide-G antagonizes rat neuronal α3β2 nicotinic acetylcholine receptor

Amandine Gaudin[1], Rómulo Aráoz[1,2*]

[1] Université Paris-Saclay, CEA, Département Médicaments et Technologies pour la Santé, SIMoS ; [2] EMR CNRS 9004, F-91191 Gif sur Yvette, France.

[*]corresponding author's email: romulo.araoz@cea.fr

Abstract

Cyclic imine toxins produced by marine dinoflagellate species move up fast the food chain through shellfish and constitute a potential threat for marine wildlife and public health because of their potent antagonistic activity against nicotinic acetylcholine receptors of muscle and neuronal types. Although not regulated, the lethality of 13-desmethyl spirolide-C does compare the lethality of saxitoxin in mouse bioassay. Besides, cyclic imine toxins are often found in shellfish destined for human consumption. Herein, the unveiling of the mode of action of cyclic imine toxins is reviewed. To illustrate the review, the electrophysiological characterization of the antagonistic capacity of 20-methyl spirolide-G on rat α3β2 nicotinic acetylcholine receptor is described.

Keywords: Cyclic imine toxins, nicotinic acetylcholine receptors, 20-methyl spirolide-G, two-electrodes voltage clamp electrophysiology (TEVC), *Xenopus laevis* oocytes

https://doi.org/10.5281/zenodo.7035152

Introduction

Cyclic imines toxins (CiTXs; ~44 members) are marine emergent neurotoxins worldwide distributed among coastal environments. Of dinoflagellate origin, CiTXs move up fast the food chain through shellfish and may constitute a potential threat for public health (Aráoz *et al*., 2020). CiTXs are potent antagonists of nicotinic acetylcholine receptors (nAChRs). They display a cyclic imine in their structure necessary for interacting with nAChRs (Bourne *et al*., 2010). Portimines (A-B) produced by *Vulcanodinium rugosum*, display a 5-membered imine ring (Selwood *et al*., 2013). The following CiTXs display a 6-membered cyclic imine ring: gymnodimines (GYM) (seven congeners), that are produced by *Karenia selliformis* and *Alexandrium peruvianum* (Seki *et al*., 1995; Van Wagoner *et al*., 2011), prorocentrolides (six members) produced by *Prorocentrum lima* (Torigoe *et al*., 1988), spiroprorocentrimine produced by *Prorocentrum* sp. (Lu *et al*., 2001), and kabirimine produced by *V. rugosum* (Hermawan *et al*., 2019). Spirolides (SPX) (16 members) produced by *A. ostenfeldii*, reviewed by Gueret and Brimble, 2010, pinnatoxins (PnTX) (A-H) produced by *V. rugosum* (Rhodes *et al*., 2010) and pteriatoxins (PtTX) (A-C) display a 7-membered cyclic imine ring (Takada *et al*., 2001).

Mode of action (MOA) of CiTXs

MOA of CiTXs from mouse assay experiments

CiTXs are fast-acting neurotoxic compounds that kill mice by respiratory arrest within minutes after intraperitoneal injection or gavage at lethal toxin doses. The clinical signs preceding mice death induced by CiTXs were similar to those evoked by curare: the administration of neostigmine, a reversible acetylcholinesterase inhibitor, increases the concentration of acetylcholine (ACh) at the neuromuscular synapse, competitively displacing curare from muscle nAChRs (Leeuwin *et al.*, 1981). Thus, the administration of two times the LD_{50} of GYM-A killed all the mice in 3-7 min. However, neostigmine pre-treated rodents survived GYM-A administration at the referred dose (Munday *et al*., 2012). This was a strong indication that muscle-type nAChR may be a molecular target of GYM-A.

Another key event was the discovery of keto-amine derivatives of SPX-A and -B, namely SPX-E and -F, in the digestive glands of scallops. The cyclic imine rings in SPX-E and -F were open and showed no activity by mouse assay. The hydrolysis of the cyclic imine ring of SPX-A and -B was associated with the presence of one methyl group on the cyclic imine ring. Thus, SPX-C, 13-desmethyl SPX-C and SPX-D were resistant to oxalic acid hydrolysis suggesting that the double methylation of the spiroimine ring confers a better chemical stability to spirolides (Hu *et al.*, 2001). SPXs (excluding SPX-A and B), PnTXs and PtTXs, have a double methylated cyclic imine ring, reviewed by Gueret and Brimble (2010) and Stivala *et al.* (2015). Further, the amino-keto PnTX-A analogue, bearing an open form of the imine ring, was inactive on muscle and neuronal nAChRs when tested by electrophysiology, confirming that the cyclic imine is critical for CiTX interaction with nAChR (Aráoz *et al.*, 2011).

MOA of CiTXs from electrophysiological research

Electrophysiological recordings using *ex vivo* neuromuscular preparations confirmed that cyclic imine toxins act on nAChRs, reviewed by Molgó *et al.* (2017). Thus, GYM-A produced a concentration- and time-dependent block of twitch responses evoked by nerve stimulation without affecting elicited muscle twitches in isolated mouse phrenic-hemidiaphragm preparations. This suggested that GYM-A blocked muscle nAChR. The reduction of the amplitude of miniature-endplate resulting from quantal ACh-release and subsequent activation of post-synaptic nAChR, confirmed the blockade of muscle-nAChR by GYM-A (Kharrat *et al.*, 2008). Similar effects on the neuromuscular junction were obtained for 13,19-desmethyl SPX-C and 13-didesmethyl SPX-C (Aráoz *et al.*, 2015; Bourne *et al.*, 2010), 20-methyl SPX-G (Couesnon *et al.*, 2016), PnTX -A, -E, -F and -G (Aráoz *et al.*, 2011; Hellyer *et al.*, 2011), and prorocentrolide-A (Amar *et al.*, 2018). These findings are consistent with *in vivo* electrophysiological recordings in sedated mice showing that a local injection of PnTX-A or PnTX-G induced the blockade of the maximal compound muscle action potential amplitude, evoked by nerve stimulation (Benoit *et al.*, 2019).

In vitro two-electrodes voltage clamp (TEVC) recordings to determine the mode of action of CiTXs were performed on *Xenopus laevis* oocytes which is a successful electrophysiological model for heterologous *de novo* expression of human ion channels and receptors and for the transplantation of membranes rich in receptors and ion channels for pharmacological studies (Miledi *et al.*, 2004). Binding of ACh to the ligand-binding sites rapidly (microseconds) shifts the receptor conformation from the resting (closed state) to the open state, initiating the ion flux through the cation-selective pore for ~2 milliseconds, and the receptor channel closes (desensitized state) (Giniatullin *et al.*, 2005). The perfusion of GYM-A, 13-desmethyl SPX-C, 13-19-didesmetyl SPX-C, 20-methyl SPX-G, PnTX-A, -E, -F, and -G or prorocentrolide does not evoke inward currents on muscle and neuronal nAChRs regardless of subtype composition or toxin concentration. When these CiTXs are co-applied with ACh, the ACh-elicited currents are inhibited in a concentration-dependent manner. The inhibition degree is dependent on the nAChR subtype and on the CiTX tested. The blockade of muscle and neuronal receptors is not voltage-dependent.

Indeed, CiTXs are competitive antagonists of muscle and neuronal nAChRs with broad subtype selectivity and high potency. Spirolides showed sub-nanomolar affinities for *Torpedo* $(\alpha1)_2\beta1\gamma\delta$ nAChR (Aráoz *et al.*, 2015), while the affinities of GYM-A and PnTX-A and -G were in the nanomolar range (Aráoz *et al.*, 2011; Kharrat *et al.*, 2008). The affinities of the studied CiTXs for human *h*α4β2 nAChRs are in the nanomolar range (Stivala *et al.*, 2015). Except for PnTX-G, GYM-A, 13-desmethyl SPX-C, 13-19 didesmethyl SPX-C, 20-methyl SPX-G and PnTX-A showed picomolar affinities for *h*α7 nAChR (Bourne *et al.*, 2015). Portimine-A and prorocentrolide-A were less active on muscle and neuronal nAChR (Amar *et al.*, 2018; Lamoise *et al.*, 2017). PnTX-A shows the best selectivity profile: the affinity of PnTX-A for α7 nAChR is 50-times higher than its affinity for *Torpedo* $(\alpha1)_2\beta1\gamma\delta$ nAChR, and 300-times higher than its affinity for α4β2 nAChR (Aráoz *et al.*, 2011).

CiTXs' target: nicotinic acetylcholine receptor

nAChRs are allosteric transmembrane pentameric proteins belonging to the cysteine-loop ligand-gated ion channel superfamily. Muscle nAChR ensures fast neurotransmission at the neuromuscular junction that is essential for respiration and muscle contraction for daily life, mobility, or scape from predation (Albuquerque *et al.*, 2009). At the central nervous system (CNS), neuronal nAChRs modulate neurotransmitters release, hence participating in fundamental aspects of synaptic plasticity involved in attention, learning, memory, and neurodegenerative disorders. Non-neuronal nAChRs are ubiquitously expressed in the human body from epithelial cells, to primary immune organs such as the bone marrow, thymus and macrophages (Bertrand *et al.*, 2015). Human genomic studies revealed 16 homologous genes coding for nAChR-subunits. The presence of the Cys-pair characterizes α subunits (α1-α10), and its absence characterize β1-β4, γ, δ and ε subunits. Muscle-nAChRs can be fetal $(\alpha1)_2\beta1\gamma\delta$ or adult $(\alpha1)_2\beta1\gamma\varepsilon$. Neuronal nAChRs show more variability resulting from the combination of α2-α7 with β2-β4 subunits. The α7 and α9 form monomeric receptors, and α8 subunit was found only in avian tissues. The heteropentameric α7β2 and α9α10 nAChRs were found in the CNS (Bertrand *et al.*, 2015). Different receptor configurations display distinct pharmacological profiles and receptor distribution patterns across the brain.

MOA of CiTXs from crystallographic studies

GYM-A & 13-desmethyl SPX-C, and PnTX-A & PnTX-G were co-crystalized with the ACh-binding

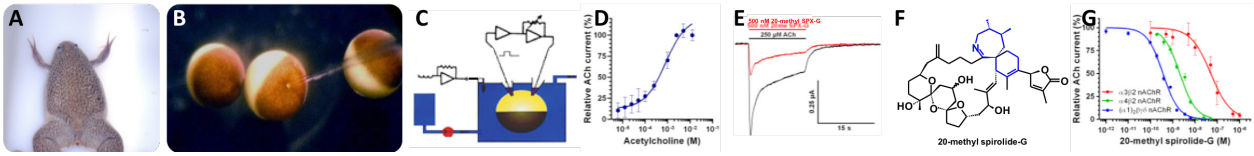

Fig. 1. MOA of 20-methyl SPX-G on *r*α3β2 nAChR. (A) *Xenopus laevis* frog. (B) *Xenopus* oocyte microinjected with mRNA. (C) Schema of TEVC: a *Xenopus* oocyte is impaled with two electrodes. ACh-evoked currents are recorded at a holding potential of -60 mV. (D) ACh dose-response curve on oocytes expressing *r*α3β2 nAChR. (E) Electrophysiological recordings showing ACh-current (black) and the antagonistic effect of 500 nM 20-methyl SPX-G (red). (F) 20-methyl SPX-G. (G) Concentration-dependent inhibition of ACh-evoked currents by 20-methyl SPX-G in *Xenopus* oocytes having incorporated *Torpedo*-(α1)2βγδ nAChR (blue), or expressing the *h*α4β2 (green) (Couesnon *et al.*, 2016), and the *r*α3β2 (red; this work). Amplitudes of the ACh-current peak (mean ± SEM; 5 oocytes per concentration), were normalized to control currents and fitted to the Hill equation.

protein from *Lymnaea stagnalis* and *Aplysia californica* to define the structural determinants responsible for their with the orthosteric site of *h*α7 nAChR, (Bourne *et al.*, 2010; 2015). These proteins are structural surrogates of the extracellular ligand-binding domain of *h*α7 nAChR. Overall, the co-crystalized CiTXs share a similar binding mode where the conserved loop C envelops the bound toxins buried at the binding interface with high surface complementary. The protonated imine nitrogen of the six- or seven-membered cyclic imines is positioned to hydrogen bond to the backbone carbonyl oxygen of loop C Trp147, a key residue for agonists and antagonists binding. The bis-spiroketal substituent of PnTX-A and PnTX-G binds between the loop C and the complementary side of the subunit interface, as observed for 13-desmethyl SPX-C and for the tetrahydrofuran group of GYM-A. The cyclohexene-butyrolactone of 13-desmethyl SPX-C interacts with Y188 and K143, while in the case of GYM-A, it interacts with Y188 and Q186. In the case of the two latter toxins, very limited interaction is observed with the sequence-variable loop F. On the contrary, the bridged ketal ring specific to PnTXs extends out of the binding pocket underneath loop C to interact with loop F on the negative side of the interface. Specific interactions between the charged carboxylate group of PnTX-A and the vinyl group of PnTX-G, may explain the selectivity towards *h*α7 and *Torpedo*-$(\alpha1)_2\beta1\gamma\delta$ nAChRs (Bourne *et al.*, 2015).

20-methyl SPX-G antagonizes rat *r*α3β2 nAChR

The α3 nAChR subunit was the first to be cloned and the α3β2 nAChR subtype was among the first subtypes to be heterologously expressed in *X. laevis* oocytes for electrophysiology (Boulter *et al.*, 1987). α3β2 nAChR is expressed in the CNS, the spinal cord and the hearth, and as presynaptic receptor in the neuromuscular junction (Young *et al.*, 2008; Fagerlund and Eriksson, 2009). The MOA of 20-methyl SPX-G (CIFGA, Spain) on α3β2 nAChRs determined by TEVC is here shown.

The mRNAs coding for the rat α3 and β2 nAChR subtypes were synthesized from the plasmids PKNΩα3 and PKNΩβ2 kindly provided by Annette Nicke (LMU, Munich, Germany), and injected into *X. laevis* oocytes (Fig. 1A-B). TEVC electrophysiology was performed as described in (Aráoz *et al.*, 2011) (Fig. 1C). The dose-response curve for ACh gave an EC_{50} of 250 µM (*n*H = 0.945 ± 0.15; Fig. 1D). The perfusion of 250 µM ACh induced a rapid opening of the α3β2 nAChR's channel (microseconds) followed by a two-phase desensitization pattern: a very fast (milliseconds) after the peak amplitude was reached and a slow desensitization phase (Fig. 1E). The perfusion of a mix containing 250 µM ACh and 20-methyl SPX-G (Figs. 1E, F) at a given concentration in the range of 100 pM – 1 µM induced a competitive blockade of the ACh-evoked currents with an IC_{50} of 50.9 nM (*n*H = -0.98 ± 0.14 Fig. 1E, 1G), without affecting the desensitization pattern of the receptor. 20-methyl SPX-G is not an agonist of α3β2 nAChR.

20-methyl SPX-G showed picomolar affinities for *Torpedo*-$(\alpha1)_2\beta1\gamma\delta$ nAChR (IC_{50} = 360 pM) and for *h*α7 nAChR (IC_{50} = 480 pM). Its affinity for the neuronal *h*α4β2 nAChR was 2.1 nM (Fig. 1G) while for rat α3β2 nAChR was 50.9 nM. Unlike *Torpedo*-$(\alpha1)_2\beta1\gamma\delta$ and *h*α7 subtypes, the β2 containing α4β2 and α3β2 nAChRs are resistant to α-bungarotoxin, but sensitive to kappa-

bungarotoxin (Boulter *et al.*, 1987). Molecular docking to predict the structural determinants within *h*α3β2 nAChR and 20-methyl SPX-G were performed (Couesnon *et al.*, 2016). Key amino acids explaining the antagonism of 20-methyl SPX-G towards *h*α3β2 and *h*α4β2 nAChRs are conserved in the orthosteric site. The lower affinity of both nAChR subtypes for 20-methyl SPX-G relies on the bulky K77 which provokes steric clashes displacing the spiroketal moiety of the toxin to the β2 subunit (Couesnon *et al.*, 2016). Further, the butyrolactone of 20-methyl SPX-G hydrogen bond with R186 of *h*α4β2 nAChR while it hydrogen bond with K143 of *r*α3β2 nAChR.

Acknowledgements. We acknowledge the funding from Labex Lermit (Detectneurotox CDE2017-001173-RD91 to RA), NRBC-E (Multitox H35 to RA) and Interreg Atlantic Area (Alertoxnet EAPA_317/2016).

References

Albuquerque, E.X., Pereira, E.F.R., Alkondon, M., Rogers S.W. (2009). Physiol. Rev. 89, 73-120.

Amar, M., Araoz, R., Iorga, B.I., *et al.,* (2018). Toxins (Basel) 10, 97.

Aráoz, R., Barnes, P., Sechet, V., *et al.,* (2020). Harmful Algae 98, 101887.

Aráoz, R., Ouanounou, G., Iorga, B. I., *et al.,* (2015). Toxicol Sci. 147, 156-167.

Aráoz, R., Servent, D., Molgó, J., *et al.,* (2011). J. Am. Chem. Soc. 133, 10499-10511.

Benoit, E., Couesnon, A., Lindovsky, J., *et al.,* (2019). Mar. Drugs 17, Article 306.

Bertrand, D., Lee, C. H., Flood, D., *et al.,* (2015). Pharmacol. Rev. 67, 1025-1073.

Boulter, J., Connolly, J., Deneris, E., *et al.,* (1987). Proc. Natl. Acad. Sci. U.S.A., 84, 7763-7767.

Bourne, Y., Radic, Z., Aráoz, R., *et al.,* (2010). Proc. Natl. Acad. Sci. U.S.A. 107, 6076-6081.

Bourne, Y., Sulzenbacher, G., Radic, Z., *et al.,* (2015). Structure 23, 1106-1115.

Couesnon, A., Aráoz, R., Iorga, B.I., *et al.,* (2016). Toxins (Basel) 8, 249.

Fagerlund, M. J. and Eriksson, L. I. (2009). Bri. J. Anaesth. 103, 108-114.

Giniatullin, R., Nistri, A., Yakel, J.L. (2005). Trends Neurosci. 28, 371-378.

Gueret, S. M. and Brimble, M. A. (2010). Nat. Prod. Rep. 27, 1350-1366.

Hellyer, S.D., Selwood, A. I., Rhodes, L., Kerr, D. S. (2011). Toxicon 58, 693-699.

Hermawan, I., Higa, M., Hutabarat, P.U.B., *et al.*, (2019). Mar. Drugs 17, Article 353.

Hu, T.M., Burton, I.W., Cembella, A.D., *et al.,* (2001). J. Nat. Prod. 64, 308-312.

Kharrat, R., Servent, D., Girard, E., *et al.,* (2008). J. Neurochem. 107, 952-963.

Lamoise, C., Gaudin, A., Hess, P., *et al.,* (2017). In: Proenza, L. and Hallegraeff, G.M. (Eds). Proc. 17th ICHA, Florianopolis, Brazil 126-129.

Leeuwin, R. S., Veldsemacurrie, R. D., Vanwilgenburg, H., *et al*., (1981). Eur. J. Pharmacol. 69, 165-173.

Lu, C.K., Lee, G.H., Huang, R., Chou, H.N. (2001). Tetrahedron Lett. 42, 1713-1716.

Miledi, R., Duenas, Z., Martinez, A., *et al.,* (2004). Proc. Natl. Acad. Sci. U.S.A. 101, 1760-1763.

Molgó, J., Marchot, P., Aráoz, R., *et al.,* (2017). J. Neurochem. 142, 41-51.

Munday, R., Selwood, A.I., Rhodes, L. (2012). Toxicon 60, 995-999.

Rhodes, L., Smith, K., Selwood, A. *et al.,* (2010). Harmful Algae 9, 384-389.

Seki, T., Satake, M., Mackenzie, L., *et al.,* (1995). Tetrahedron Lett. 36, 7093-7096.

Selwood, A. I., Wilkins, A. L., Munday, R., *et al.,* (2013). Tetrahedron Lett. 54, 4705-4707.

Stivala, C.E., Benoit, E., Aráoz, R., *et al.,* (2015). Nat. Prod. Rep. 32, 411-435.

Takada, N., Umemura, N., Suenaga, K., Uemura, D. (2001). Tetrahedron Lett. 42, 3495-3497.

Torigoe, K., Murata, M., Yasumoto, T., Iwashita, T. (1988). J.A.C.S. 110, 7876-7877.

Van Wagoner, R.M., Misner, I., Tomas, C.R., *et al.,* (2011). Tetrahedron Lett. 52, 4243-4246.

Young, T., Wittenauer, S., McIntosh, J.M., *et al.,* (2008). Brain Res. 1229, 118-124.